Influence of baryons on the spatial distribution of matter: higher order correlation functions *

Xiao-Jun Zhu[1] and Jun Pan[1,2]

[1] Purple Mountain Observatory, Chinese Academy of Sciences, Nanjing 210008, China;
   zhuxiaojun1985@gmail.com
[2] National Astronomical Observatories, Chinese Academy of Sciences, Beijing 100012, China

Abstract Physical processes involving baryons could leave a non-negligible imprint on the distribution of cosmic matter. A series of simulated data sets at high resolution with identical initial conditions are employed for count-in-cell analysis, including one N-body pure dark matter run, one with only adiabatic gas and one with dissipative processes. Variances and higher order cumulants S_n of dark matter and gas are estimated. It is found that physical processes with baryons mainly affect distributions of dark matter at scales less than $1\ h^{-1}$ Mpc. In comparison with the pure dark matter run, adiabatic processes alone strengthen the variance of dark matter by $\sim 10\%$ at a scale of $0.1\ h^{-1}$ Mpc, while the S_n parameters of dark matter only mildly deviate by a few percent. The dissipative gas run does not differ much from the adiabatic run in terms of variance for dark matter, but renders significantly different S_n parameters describing the dark matter, bringing about a more than 10% enhancement to S_3 at $0.1\ h^{-1}$ Mpc and $z = 0$ and being even larger at a higher redshift. Distribution patterns of gas in two hydrodynamical simulations are quite different. Variance of gas at $z = 0$ decreases by $\sim 30\%$ in the adiabatic simulation but by $\sim 60\%$ in the non-adiabatic simulation at $0.1\ h^{-1}$ Mpc. The attenuation is weaker at larger scales but is still obvious at $\sim 10\ h^{-1}$ Mpc. S_n parameters of gas are biased upward at scales $<\sim 4\ h^{-1}$ Mpc, and dissipative processes show an $\sim 84\%$ promotion at $z = 0$ to S_3 at $0.1\ h^{-1}$ Mpc in contrast with the $\sim 7\%$ change in the adiabatic run. The segregation in clustering between gas and dark matter could have dramatic implications on modeling distributions of galaxies and relevant cosmological applications demanding fine details of matter distribution in a strongly nonlinear regime.

Key words: cosmology: dark matter — large-scale structure of universe — methods: statistical

1 INTRODUCTION

The present clustering pattern of large scale structures on cosmological scales is generally interpreted as the growth of primordial density fluctuations, mainly through gravitational instability of dark matter which dominates the matter content of the Universe. Although at large scales the gravitational

monodrama of dark matter is well understood, at small scales ignoring non-gravitational effects associated with galaxy formation would induce considerable systematics to the relevant application. Quantification of such an impact of baryons, including scale range and strength, is strongly desired to meet the accuracy budget of cosmological parameter estimation (e.g. Shaw et al. 2010; Semboloni et al. 2011), structure formationand refinement of the evolution model (e.g. Stanek et al. 2009; Dolag et al. 2009).

In contrast to the simplicity of gravitational force, the physical processes that baryons are involved in, such as radiative cooling and star formation, are usually very complicated and highly entangled. Even worse is that physical processes for baryons normally operate in a strongly nonlinear regime where gravitational evolution is already analytically intractable. Advanced computational facilities and algorithms, together with accumulated knowledge summarized from modern observations, have enabled high resolution hydrodynamic simulations with various treatment prescriptions for baryon physics plugged in (e.g. Teyssier 2002; Springel 2005). To date, investigations on the effects of different physical processes for baryons are carried out mainly with numerical simulations (e.g. van Daalen et al. 2011), though there is still a long way to go to build trustworthy machinery that captures the messy gas physics in full detail.

Recent analysis of simulated data sets has shown that baryonic physical processes could alter the power spectrum of matter at $k > 10\,h\,\mathrm{Mpc}^{-1}$ and consequently the weak lensing power spectrum by some non-negligible percentage (Jing et al. 2006), which is confirmed and greatly extended in later works (e.g. Rudd et al. 2008; Hearin & Zentner 2009; van Daalen et al. 2011; Semboloni et al. 2011; Casarini et al. 2012). The modulation to the power spectrum at such small scales, speaking in the terminology of halos for matter clustering, is mainly based upon the one-halo term which is only determined by mass distribution inside halos and the halo mass distribution function (Cooray & Sheth 2002). The presence of gas in simulations does slightly boost the concentration parameter of the halo mass profile (Lin et al. 2006) and measurably affects the high mass branch of the halo mass function (Stanek et al. 2009; Cui et al. 2012), even with adiabatic processes alone. Such changes in halo properties can actually bring about a significant alteration to strong lensing statistics (Wambsganss et al. 2008) and the thermal and kinetic Sunyaev-Zel'dovich power spectrum (Battaglia et al. 2010; Shaw et al. 2010) as well.

The basic scenario here is that baryons are directly redistributed by adiabatic contraction, radiative cooling, various feedbacks from galaxies and their central black holes, and star formation activities etc. Then, the distribution of dark matter is modified through gravitational coupling with baryons. Since dark matter and baryons experience different interactions, it is normal to expect that their clustering would differ from the pattern shown in the dark matter only case in a complex way.

In the work of Jing et al. (2006), it is found that the clustering of the gas is suppressed but that of dark matter is boosted at scales $k > 1\,h\,\mathrm{Mpc}^{-1}$, resulting in the clustering of total matter being suppressed at a level of 1% at $1 < k < 10\,h\,\mathrm{Mpc}^{-1}$ but then boosted up to 2% in the nonradiative run and 10% in the run with star formation at $k \approx 20\,h\,\mathrm{Mpc}^{-1}$. Extensive research by van Daalen et al. (2011) with AGN feedback provided a quantitatively different description, due to their different implementations of gas physics, though it is still qualitatively in agreement with Jing et al. (2006). They discovered that the 1% decrease in the power spectrum of total matter at $z = 0$ compared to that of the pure dark matter simulation can be as low as $k \sim 0.3\,h\,\mathrm{Mpc}^{-1}$, a 10% drop appears at $k \sim 10\,h\,\mathrm{Mpc}^{-1}$, and an enhancement in clustering is observed at $k > \sim 70\,h\,\mathrm{Mpc}^{-1}$. Compared with the power spectrum of the pure dark matter run, gas in hydrodynamic simulations exhibits much less power in the case of $k > 1\,h\,\mathrm{Mpc}^{-1}$, but the dark matter component shows a power boost at $k > 10\,h\,\mathrm{Mpc}^{-1}$.

The influence of baryons on matter clustering and the segregation of baryons from dark matter in clustering can be better observed with higher order correlation functions which are known to be able to reveal more subtle details of clustering than two-point statistics like the power spectrum. Guillet

et al. (2010) measured the skewness of the MareNostrum simulation[1] and also a set of simulations with only dark matter. They found that, compared to the distribution of matter in the pure dark matter simulation, in the hydrodynamic simulation the dark matter component shows mildly decreased skewness between $0.3 < r < 1 \, h^{-1}$ Mpc and then apparently becomes boosted at smaller scales. They demonstrated that by adding an exponential gaseous disk profile to the halo model, they could roughly reproduce their measurements.

In this paper we perform count-in-cell measurements of N-body/SPH simulations together with a pure dark matter simulation as a reference, in order to better depict the impact of gas physics on matter distribution at higher orders to complement works based on the power spectrum, and which also serves as an independent check to the results of Guillet et al. (2010). Furthermore, our interests are particularly on the phenomenon of segregation between gas and dark matter, i.e. the differences in distribution among types of matter, which might cast light on the origin of the galaxy bias. The layout of the paper is as follows: Section 2 contains a description of the simulation data and an estimation method for the higher order correlation function. The results and their analysis are in Section 3. The last section is for the summary and discussion.

2 COUNT-IN-CELL MEASUREMENTS OF SIMULATED DATA

2.1 The Simulations

The simulated data sets we use are the same as in Jing et al. (2006), which consist of three simulations produced by the GADGET2 code (Springel 2005), one pure dark matter simulation, one hydrodynamic simulation with only adiabatic processes, and one hydrodynamic simulation that incorporates radiative cooling, star formation, and supernovae feedback *etc.* The three simulations are run with 512^3 particles for each component of dark matter and gas, starting at $z_{\mathrm{ini}} = 120$ with the same initial condition in a cubic box of $100 \, h^{-1}$ Mpc, and their cosmological parameters are set to $(\Omega_m, \Omega_\Lambda, \Omega_b, \sigma_8, n, h)$=$(0.268, 0.732, 0.044, 0.85, 1, 0.71)$. More details about the simulations can be found in Jing et al. (2006) and Lin et al. (2006). Here, three snapshots at $z = 0, 0.526$ and 1.442 are selected for analysis.

2.2 Count-in-cell and Higher Order Correlation Functions

In this study, higher order correlation functions are those that are volume averaged, i.e. higher order connected moments of smoothed density fluctuation fields δ by a certain window function w, with $\bar{\xi}_n = \langle \delta^n \rangle_{\mathrm{c}}$. $\bar{\xi}_n$ can be estimated through the count probability distribution function $P_N(R)$ by the count-in-cell method. Given a cubic cell with side size R, P_N at this scale is the probability that a randomly selected cell in the catalog contains N galaxies,

$$P_N = \frac{1}{C} \sum_{i=1}^{C} \delta_D(N_i = N) \, . \tag{1}$$

Under the usual local Poisson approximation, P_N is the probability distribution function $p(\delta)$ of a smoothed density fluctuation convolved with a Poisson kernel (see the review of Bernardeau et al. 2002)

$$P_N = \int_{-1}^{+\infty} p(\delta) \frac{[\langle N \rangle (1 + \delta)]^N \mathrm{e}^{-\langle N \rangle (1+\delta)}}{N!} d\delta \, , \tag{2}$$

---

[1] *http://astro.ft.unam.es/~marenostrum*

where $\langle N \rangle$ is the mean count-in-cell. Higher order correlation functions $\overline{\xi}_n$ are often expressed by the hierarchy of higher order cumulants S_n,

$$S_n = \frac{\overline{\xi}_n}{\overline{\xi}_2^{n-1}}, \tag{3}$$

which can be derived from the following recursion relation

$$S_n = \frac{\overline{\xi}_2 F_n}{N_c^n} - \frac{1}{n} \sum_{k=1}^{n-1} \binom{n}{k} \frac{(n-k)S_{n-k}F_k}{N_c^k}, \tag{4}$$

where $N_c = \langle N \rangle \overline{\xi}_2$ and the factorial moments

$$F_k = \sum P_N(R) \times (N)_k = \langle N(N-1)\dots(N-k+1) \rangle. \tag{5}$$

Explicit estimators for the variance, skewness and kurtosis are just

$$\begin{aligned}
\overline{\xi}_2 &= \frac{F_2}{F_1^2} - 1, \\
S_3 &= \frac{F_1(F_3 - 3F_1F_2 + 2F_1^3)}{(F_2 - F_1^2)^2}, \\
S_4 &= \frac{F_1^2(F_4 - 4F_3F_1 - 3F_2^2 + 12F_2F_1^2 - 6F_1^4)}{(F_2 - F_1^2)^3}.
\end{aligned} \tag{6}$$

P_N is calculated with the over-sampling algorithm to reach a sampling rate of $\sim 10^7$ (Szapudi 1998). Probing scale R is limited to be within $(0.1, 10)\ h^{-1}$ Mpc; the small scale cut is chosen so as to ensure robust recovery of statistics over discreteness (normally $\langle N \rangle > 0.1$ is sufficient), and the large scale limit comes from above one-tenth of the box size, at which correlation functions are no longer reliable by practical experience. Since all simulations are evolved from the same initial conditions, in the same volume and with the same resolution, there is no need to calculate their cosmic variance (or error bars) if we are simply interested in their differences.

3 INFLUENCE OF BARYONIC PHYSICS ON CLUSTERING

3.1 Clustering of Dark Matter

Correlation functions of dark matter in three simulation runs are illustrated in Figure 1, showing their respective redshift evolutions. It has been checked that if we rescale $\overline{\xi}_2$ with $D(z)$, the growth rate of large scale structure (see Lahav et al. 1991, for approximate formula), variances at different redshift are in good agreement at scales where $\overline{\xi}_2(R, z = 0) < 1$; it is well known that at smaller scales $\overline{\xi}_2(z)D^2(z=0)/D^2(z)$ becomes lower with increasing z.

S_n parameters are apparently larger at higher redshift with scales $R <\sim 3\ h^{-1}$ Mpc, and the decrement from $z = 1.442$ to $z = 0.526$ in S_n parameters is much bigger than that from $z = 0.526$ to $z = 0$. Recall that $\overline{\xi}_{n>2}$ terms are measures of non-Gaussianity and our simulations are evolved from Gaussian initial conditions. Intuitively, non-Gaussianity would increase when the redshift decreases, in line with the growth of gravitational nonlinearity. Let the cosmic scale factor $a = 1/(1+z)$ and $\Delta a > 0$ be a small increment to a, as

$$S_n(a + \Delta a) < S_n(a), \qquad S_n = \overline{\xi}_n/\overline{\xi}_2^{n-1}, \qquad \overline{\xi}_n(a + \Delta a) > \overline{\xi}_n(a),$$
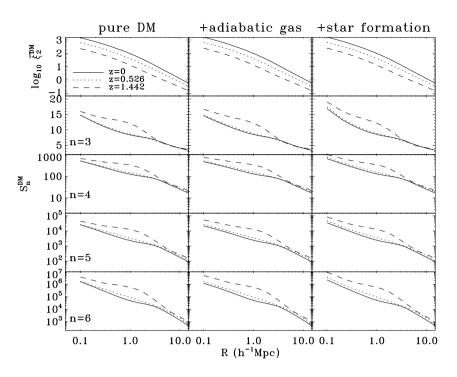
Fig. 1 $\overline{\xi}_2$ and $S_n = \overline{\xi}_n/\overline{\xi}_2^{n-1}$ up to $n = 6$ for dark matter in simulation runs of pure dark matter (*left*), with adiabatic gas physics only (*middle*), and with star formation and other gas physics (*right*). Solid, dotted and dashed lines are for $z = 0, 0.526$ and 1.442 respectively.

and at small scales $\overline{\xi}_n > 0$, there is

$$\log \overline{\xi}_n(a + \Delta a) - \log \overline{\xi}_n(a) < (n - 1) \left[\log \overline{\xi}_2(a + \Delta a) - \log \overline{\xi}_2(a)\right] \; , \tag{7}$$

so that subsequently

$$\frac{d \log \overline{\xi}_n}{d \log a} < (n - 1)\frac{d \log \overline{\xi}_2}{d \log a} \; , \quad \text{for } n > 2 \; , \tag{8}$$

which establishes an interesting relationship between the evolution rates of higher order correlation functions and that of the two point correlation function in a strongly nonlinear regime.

At scales $R >\sim 3 \; h^{-1}$ Mpc, S_n terms show little dependence on redshift, so $S_n(a < 1) \approx S_n(a = 1)$ is used as the predicted perturbation theory (Fosalba & Gaztanaga 1998). However, the approximation is not perfect in our raw results, since at large scales there are differences at different epochs at a level of a few percent. S_n values at a higher redshift turn out to be slightly larger. It is known that there is a problem rooted in the Zel'dovich approximation based on the way initial conditions are generated. The resulting correction to measured S_n at leading order decays with the redshift at a rate roughly $\propto [D(z)/D(z_{\mathrm{ini}})]^{-1}$. But the effect of the bias is that true values of S_n are larger than the measured ones (Scoccimarro 1998; Fosalba & Gaztanaga 1998), so that the offsets between different redshifts will be even higher than what is shown in Figure 1. The puzzle could be dynamical rather than systematical biases. Here we just leave the issue to future work.

The influence of gas physics on the distribution of dark matter is displayed in Figure 2. Enhancement to $\overline{\xi}_2$ induced by gas is mild and increases to $\sim 10\%$ at $\sim 0.1 \; h^{-1}$ Mpc, which is consistent with previous works (e.g. Jing et al. 2006; Guillet et al. 2010). Gas physics other than
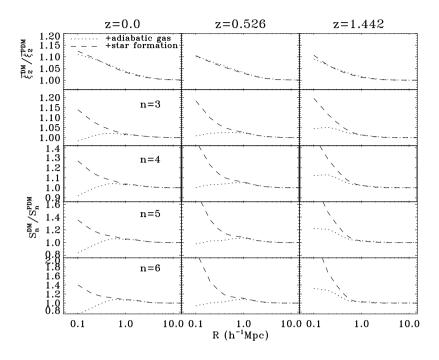
Fig. 2 Influence of gas physics on the distribution of dark matter: ratios of correlation functions of dark matter in hydrodynamical simulations to those of dark matter in the pure dark matter simulation.

the adiabatic process does not introduce significant extra modulation to the two point correlation function of dark matter, but their effects are seen in higher order functions.

From Figure 2 it is clear that dark matter clustering is immune to baryons at large scales, and the stage at which gas physics plays a part is mainly on scales $R <\sim 1\ h^{-1}$ Mpc. In the adiabatic run, at $z = 1.442$, S_n^{DM}/S_n^{PDM} only becomes larger than one on scales smaller than $1\ h^{-1}$ Mpc. It is smaller at $z = 0.526$, then the boost switches to suppression at scales $< 0.2\ h^{-1}$ Mpc. The level of impact is not very large; at $0.1\ h^{-1}$ Mpc skewness S_3 is increased by $\sim 5\%$ at $z = 1.442$ and then decreased by $\sim 2\%$ at $z = 0$, and variation in kurtosis at such a scale is $\sim +12\%$ at $z = 1.442$ but $\sim -8\%$ at $z = 0$.

Effects of star formation activities and other gas physics are much stronger than the adiabatic process, with amplitudes of S_n at all redshift being raised significantly, however the increment decreases at a lower redshift, for instance the relative enhancement to S_3 and S_4 at $R = 0.1\ h^{-1}$ Mpc is $\sim 20\%$ and $\sim 52\%$ at $z = 1.442$, but drops down to $\sim 14\%$ and $\sim 27\%$ at $z = 0$ respectively. It appears that if we are about to investigate differences among models built with different baryonic processes through cluster analysis of dark matter, we should concentrate on higher order statistics on sub-mega parsec scales, and preferentially at a higher redshift.

3.2 Clustering of Baryonic Gas

Correlation functions of gas are presented in Figure 3. Redshift evolution from correlation functions of gas in the adiabatic simulation is similar to the dark matter component as in Figure 1, with S_n being larger at higher redshift at scales less than $\sim 3\ h^{-1}$ Mpc. There is more complexity in the non-adiabatic hydrodynamic simulation. The S_n parameters have more complicated behavior at scales $<\sim 0.2\ h^{-1}$ Mpc, which is probably a reflection of the composite action from competing physical
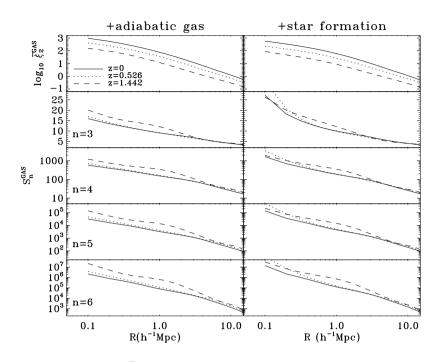
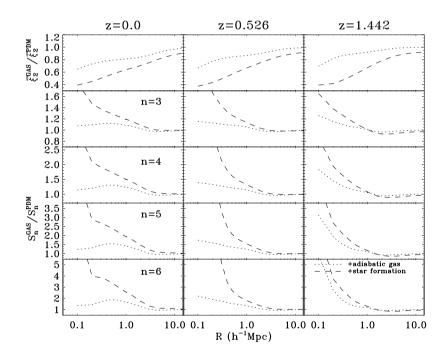**Fig. 3** $\overline{\xi}_2$ and S_n of gas in hydrodynamic simulations.

Fig. 4 Comparison of correlation functions of gas in hydrodynamic simulations to those of dark matter in the pure dark matter run.
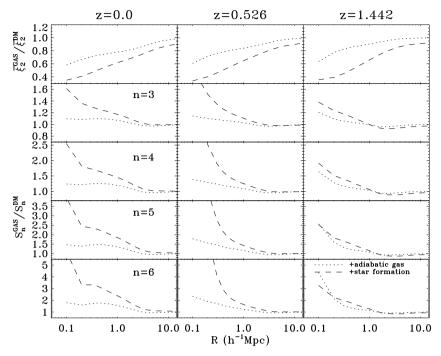
Fig. 5 Differences between distributions of gas and dark matter in hydrodynamic simulations.

processes involving gas, e.g. radiative cooling versus feedbacks from supernovae. To separate the effect of individual components of gas physics, a series of simulations with different prescriptions is definitely needed, similar to the work of van Daalen et al. (2011).

In hydrodynamical simulations, the distribution of gas more obviously deviates from that of dark matter in the simulation with pure dark matter than its counterpart (Fig. 4), in terms of both amplitude of correlation functions and affected scale range, and again the effects become weaker at a lower redshift. All S_n values of gas are boosted significantly at scales $<\sim 4\ h^{-1}$ Mpc, in agreement with Jing et al. (2006) where variance of gas $\bar{\xi}_2$ is dramatically smaller on fairly broad scales extending to around $10\ h^{-1}$ Mpc. At $z = 0$, $\bar{\xi}_2$ decreases by $\sim 30\%$ in the adiabatic simulation but by $\sim 60\%$ in the non-adiabatic simulation at $0.1\ h^{-1}$ Mpc. Bifurcation due to differences in the physical mechanisms of gas employed in simulations is also observed. Non-adiabatic gas physics induces stronger variation to the clustering of matter; there is an $\sim 84\%$ and $\sim 220\%$ increase at $z = 0$ to S_3 and S_4 respectively at $0.1\ h^{-1}$ Mpc but only a moderate $\sim 7\%$ and $\sim 14\%$ gain in the adiabatic simulation.

3.3 Segregation of Clustering for Gas and Dark Matter

It is now clear that including gas can result in different distribution patterns, for both dark matter and gas compared to pure dark matter, at very small scales. From the results shown above it appears that the distribution of gas is more severely affected than that of dark matter, which is easy to understand as gas is directly affected by complex physics, but dark matter is influenced only through its gravitational coupling to baryons. A direct comparison of correlation functions for gas with dark matter is shown in Figure 5. We can see that for the two point correlation function, differences appear at scales as large as $\sim 10\ h^{-1}$ Mpc, but for higher order cumulants the departure scale is $\sim 4\ h^{-1}$ Mpc.

The volume averaged two point correlation function of gas is obviously lower than the one for dark matter. At $0.1\ h^{-1}$ Mpc the gap could be as large as $\sim 40\% - 60\%$; in the adiabatic run the difference at $z = 0$ is already around 20% at $1\ h^{-1}$ Mpc and in the non-adiabatic run it becomes $\sim 40\%$ at such a scale. However, S_n parameters of gas are much larger than those of dark matter, for example at $0.1\ h^{-1}$ Mpc enhancement to the skewness S_3 at $z = 0$ is about 10% in the adiabatic run and $\sim 62\%$ in the non-adiabatic run. The results indicate that the distribution of gas has a longer tail than that of dark matter. In another words, there are more highly concentrated small clumps of gas than dark matter.

The bias of gas compared to dark matter in terms of S_n at $z = 0.526$ is largest in both hydrodynamic simulations. We conjecture that the effects of gas physics must reach a peak at a redshift $z > 0$ and then relax after that, entering a more passive stage of evolution. If the rate of galaxy assembly is strongly correlated with the accumulated effect of gas physics, it is likely that there would be an apex within that time interval. Of course, the exact peak time depends on how the baryon processes proceed.

4 SUMMARY AND DISCUSSION

In this paper, correlation functions up to sixth order are estimated from count-in-cell analysis of dark matter and gas in three simulations: the pure dark matter run, the run with the adiabatic gas process, and the one with star formation activities and other gas physics. Major results about the influence on matter clustering are the following.

(1) Compared with the case of pure dark matter, physical processes involving baryons introduce non-negligible modulation to the clustering of dark matter, and the affected regime for dark matter is at scales less than $1\ h^{-1}$ Mpc. The adiabatic process alone strengthens $\bar{\xi}_2$ by $\sim 10\%$ at a scale of $0.1\ h^{-1}$ Mpc, which is insensitive to redshift; S_n parameters in the run deviate from the pure dark matter results rather mildly, at $0.1\ h^{-1}$ Mpc skewness S_3 evolves from $\sim 5\%$ lifting at $z = 1.442$ to $\sim 2\%$ falling at $z = 0$. Meanwhile, the difference in kurtosis S_4 changes from $\sim 12\%$ to negative $\sim -8\%$. In the run with dissipative gas processes, $\bar{\xi}_2$ does not differ much from the adiabatic run, but S_n parameters all significantly increase, adding $\sim 14\%$ to S_3 and $\sim 27\%$ to S_4 at $0.1\ h^{-1}$ Mpc and $z = 0$, and the amplitude of change is larger at a higher redshift.

(2) Gas distribution in hydrodynamic simulations is much more strongly modified than the dark matter component. A two point correlation function of gas at $z = 0$ decreases by $\sim 30\%$ in an adiabatic simulation, but by $\sim 60\%$ in a non-adiabatic simulation at $0.1\ h^{-1}$ Mpc. The attenuation is weaker at larger scales but is still obvious at $\sim 10\ h^{-1}$ Mpc. S_n parameters of gas are biased upward at scales $< \sim 4\ h^{-1}$ Mpc, and dissipative processes add significantly more power to them, giving an $\sim 84\%$ promotion at $z = 0$ to S_3 at $0.1\ h^{-1}$ Mpc against the moderate $\sim 7\%$ increase in the adiabatic simulation.

(3) There is segregation of clusters between gas and dark matter in the same simulation. $\bar{\xi}_2$ of gas is already lower than its dark matter counterpart at $\sim 10\ h^{-1}$ Mpc, which is down at $0.1\ h^{-1}$ Mpc by $\sim 40\%$ and $\sim 62\%$ in the adiabatic run and the non-adiabatic run respectively. S_n terms of gas are larger than those of dark matter at scales $< 4\ h^{-1}$ Mpc. S_3 of gas in the adiabatic run increases by $\sim 10\%$ but by $\sim 60\%$ in the non-adiabatic run at $0.1\ h^{-1}$ Mpc. Biasing of gas to dark matter is much stronger in the non-adiabatic simulation than the adiabatic only run, and the maximal bias is achieved at a certain redshift $z > 0$.

It is shown in this work that differences in the distribution of dark matter that originate from various mechanisms of gas physics cannot be effectively distinguished at the second order level, though an apparent discrepancy appears in the gas. This would benefit those applications which only

rely on second order statistical properties of dark matter, but once going to higher orders one has to consider the systematics introduced by gas.

Biasing of gas to dark matter is a more interesting problem, aside from it being a serious challenge to precision cosmology such as the modeling of the Sunyaev-Zel'dovich effects (e.g. Shaw et al. 2010; Battaglia et al. 2010). We know that galaxies are biased tracers of the distribution of dark matter, but galaxies are in fact products of gas physics. It is probably more reasonable to assume that galaxies are actually tracing gas instead of dark matter. We conjecture that by the decomposition, the stochasticity and nonlinearity of galaxy bias would be greatly reduced. Standard methods exploring the relationship between galaxies and their host halos, such as the halo occupation distribution model (Berlind & Weinberg 2002) and the conditional luminosity function model (Yang et al. 2003), generally use the two point correlation function summarized from the pure dark matter simulation as a reference to the measured galaxy two point correlation function. Data points of the galaxy two point correlation function are usually at scales from $\sim 0.1\ h^{-1}$ Mpc to a few mega parsecs within which unfortunately the matter distribution underlying the galaxies is not the same as in the pure dark matter universe. We might have to quantify the amplitude of this kind of systematical bias before presenting an estimation of the number of a particular type of galaxies in halos.

References

Battaglia, N., Bond, J. R., Pfrommer, C., Sievers, J. L., & Sijacki, D. 2010, ApJ, 725, 91
Berlind, A. A., & Weinberg, D. H. 2002, ApJ, 575, 587
Bernardeau, F., Colombi, S., Gaztañaga, E., & Scoccimarro, R. 2002, Phys. Rep., 367, 1
Casarini, L., Bonometto, S. A., Borgani, S., et al. 2012, A&A, 542, A126
Cooray, A., & Sheth, R. 2002, Phys. Rep., 372, 1
Cui, W., Borgani, S., Dolag, K., Murante, G., & Tornatore, L. 2012, MNRAS, 423, 2279
Dolag, K., Borgani, S., Murante, G., & Springel, V. 2009, MNRAS, 399, 497
Fosalba, P., & Gaztanaga, E. 1998, MNRAS, 301, 503
Guillet, T., Teyssier, R., & Colombi, S. 2010, MNRAS, 405, 525
Hearin, A. P., & Zentner, A. R. 2009, J. Cosmol. Astropart. Phys., 4, 32
Jing, Y. P., Zhang, P., Lin, W. P., Gao, L., & Springel, V. 2006, ApJ, 640, L119
Lahav, O., Lilje, P. B., Primack, J. R., & Rees, M. J. 1991, MNRAS, 251, 128
Lin, W. P., Jing, Y. P., Mao, S., Gao, L., & McCarthy, I. G. 2006, ApJ, 651, 636
Rudd, D. H., Zentner, A. R., & Kravtsov, A. V. 2008, ApJ, 672, 19
Scoccimarro, R. 1998, MNRAS, 299, 1097
Semboloni, E., Hoekstra, H., Schaye, J., van Daalen, M. P., & McCarthy, I. G. 2011, MNRAS, 417, 2020
Shaw, L. D., Nagai, D., Bhattacharya, S., & Lau, E. T. 2010, ApJ, 725, 1452
Springel, V. 2005, MNRAS, 364, 1105
Stanek, R., Rudd, D., & Evrard, A. E. 2009, MNRAS, 394, L11
Szapudi, I. 1998, ApJ, 497, 16
Teyssier, R. 2002, A&A, 385, 337
van Daalen, M. P., Schaye, J., Booth, C. M., & Dalla Vecchia, C. 2011, MNRAS, 415, 3649
Wambsganss, J., Ostriker, J. P., & Bode, P. 2008, ApJ, 676, 753
Yang, X., Mo, H. J., & van den Bosch, F. C. 2003, MNRAS, 339, 1057